Biotechnol Lett
https://doi.org/10.1007/s10529-021-03085-2

ORIGINAL RESEARCH PAPER

Co-delivery of miRNA-15a and miRNA-16–1 using cationic PEGylated niosomes downregulates Bcl-2 and induces apoptosis in prostate cancer cells

Maedeh Ghaffari · Seyed Mehdi Kalantar · Mahdie Hemati · Ali Dehghani Firoozabadi · Amir Asri · Ali Shams · Sina Jafari Ghalekohneh · Fateme Haghiralsadat

Received: 29 August 2020 / Accepted: 13 January 2021

Abstract
Objective Tumor suppressor miRNAs, miR-15a and miR-16–1, with high-specificity and oncogenic targeting of Bcl-2, can target tumor tissues. Disadvantages of the clinical application of free miRNAs include poor cellular uptake and instability in plasma, which can be partially improved by using nanocarriers to deliver anti-cancer agents to the tumor cell.
Method In this study, cationic niosomes were designed and optimized with the specific formulation. Then, the physical characteristics, the cytotoxicity, the impact of transfected miRNAs on the expression of the Bcl-2 gene, and the apoptosis rate of the different formulation into prostate cancer cell were determined.
Results The optimum formulation containing tween-60: cholesterol: DOTAP: DSPE-PEG2000 at 70:30:25:5 demonstrated that the vesicle size and zeta potentials were 69.7 nm and + 14.83 mV, respectively. Additionally, noisome-loaded miRNAs had higher toxicity against cancer cells comparing with

M. Ghaffari
Department of Genetics, School of Medicine, Shahid Sadoughi University of Medical Sciences, Yazd, Iran

S. M. Kalantar
Genetic and Reproductive Unit, Recurrent Abortion Research Centre, Yazd Reproductive Sciences Institute, Shahid Sadoughi University of Medical Sciences, Yazd, Iran

M. Hemati · F. Haghiralsadat (✉)
Medical Nanotechnology and Tissue Engineering Research Center, Yazd Reproductive Sciences Institute, Shahid Sadoughi University of Medical Sciences, Yazd, Iran
e-mail: fhaghirosadat@gmail.com

M. Hemati
Department of Clinical Biochemistry, Faculty of Medicine, Shahid Sadoughi University of Medical Sciences, Yazd, Iran

A. Dehghani Firoozabadi
Yazd Cardiovascular Research Center, Shahid Sadoughi University of Medical Sciences, Yazd, Iran

A. Asri
Department of Hematology and Blood Banking, Faculty of Allied Medicine, Iran University of Medical Sciences, Tehran, Iran

A. Shams
Immunology Department, Faculty of Medicine, Shahid Sadoughi University of Medical Sciences, Yazd, Iran

S. Jafari Ghalekohneh
Department of Mechanical Engineering, University of Tehran, Tehran, Iran

F. Haghiralsadat
Department of Advanced Medical Sciences and Technologies, School of Paramedicine, Shahid Sadoughi University of Medical Sciences, Yazd, Iran

Published online: 30 January 2021

free forms. The transfection of PC3 cells with the combination therapy of nanocarriers loaded of two miRNAs led to a significant decrease in the expression of the Bcl-2 gene and increased the degree of cell death in PC3 cells compared with other treatment groups, and the synergistic effects of co-delivery of miR-15a and miR-16–1 on prostate cancer cells were shown.

Conclusion According to the results, it seems the designed niosomes containing miR-15a and miR-16–1 can target the Bcl-2 gene and provide a cheap, applicable, cost-effective, and safe drug delivery system against prostate cancer.

Keywords Prostate cancer · Nanocarrier · Bcl-2 · Apoptosis · miR-15a · miR-16–1 · Niosome

Introduction

Prostate cancer, which is considered an aggressive neoplasm, is one of the most common types of cancer diagnosed in male gender and its incidence is exponentially increased in numerous countries. The median age of the patients at the time of diagnosis is 72 years. (Kopper and Tímár 2005; Pejin et al. 2013). In many cases, there is no bona fide treatment in place when patients were diagnosed in advanced stages, because tumors in advanced and metastatic stages are very resistant to conventional chemotherapeutic agents. Consequently, it would be crucial to recognize the molecular mechanisms underlying the development of cancer to seek new therapies to fight cancer therapies. To achieve this purpose and overcome drug resistance, natural products along with chemotherapeutic agents have a special place in cancer therapy (Pejin et al. 2015). On the other hand, gene therapy by the RNA interference (RNAi) technique is a promising and unique method that interferes with the expression of particular genes and silences the genes at the transcriptional level. In this approach, small interfering RNAs (siRNA) or microRNAs (miRNA) transfect tumor cells, thus changing the expression of specific genes at the post-translational stage (Haghiralsadat et al. 2018c). Recently, the delivery of miRNAs (miRNAs) to tumor cells in order to eliminate them has attracted much attention and used in in-vitro and in-vivo studies (Guo and Wang 2019; Zhu et al. 2019). MiRNAs are non-coding and single-strand RNAs that comprise of $\sim$ 22 nucleotides and act as intracellular modulators of the gene expression. Studies have shown that the dysregulation of miRNAs is associated with the pathogenesis of different types of cancers(Palanichamy and Rao 2014). MiR-15a and miR-16–1 are categorized as the tumor suppressor microRNAs that can regulate a group of oncogenes (Aqeilan et al. 2010). However, they are usually deleted or downregulated in some types of human cancers, such as chronic lymphocytic leukemia (CLL) (Acunzo and Croce 2016), breast cancer (Patel et al. 2016), hepatocarcinoma (Zhang et al. 2010), non-small cell lung carcinoma (Bandi et al. 2009), gastric cancer (Kang et al. 2015), and prostatic cancer (Porkka et al. 2011). Both miR-15a and miR16-1 are capable of targeting multiple genes, such as Bcl-2, CCND1, MCL-1, and WNT3A (Aqeilan et al. 2009; Cai et al. 2012; Cimmino et al. 2005; Liu et al. 2014). Hence, by silencing anti-apoptotic genes, they can induce cell death, inhibit cell growth, and arrest the proliferation of malignant cells. A wide variety of cancer cells, such as prostate cancer cells apply different strategies to escape cell death, such as the upregulation of anti-apoptosis signaling pathways. Therefore, silencing the anti-apoptotic Bcl-2 gene by the application of miR-15a and miR-16–1 results in the downregulation of Bcl-2 gene expression and increases the rate of apoptosis (Chen et al. 2006; Cimmino et al. 2005). Since the simultaneous use of miR-15a and miR-16–1 shows a potent onco-suppressor activity, the synergistic use of these miRNAs can have tremendous effects on the oppression of cancer cell growth. Regarding the above evidence, the co-delivery of these two miRNAs could be a novel therapeutic option for advanced stages of prostate cancer(Bonci et al. 2008). Previous studies have indicated that the clinical application of miRNAs has some limitations since the rate of cellular uptake is very low, and these RNA molecules are easily degraded by RNAase enzymes found in the bloodstream (Baraban et al. 2018; Qian et al. 2017). Therefore, the development of a suitable carrier system to be able to protect and stabilize miRNAs is an urgent need for the efficient delivery to cancer cells. Among carriers employed for the transfection of cells by RNAi, cationic lipids are useful and effective carriers for the delivery of polyanionic molecules, such as RNA and DNA (Haghiralsadat et al. 2018b; Hsu et al. 2013). In comparison with other

types of carriers, cationic lipids are safe (low immunogenicity) and readily prepared and used. Besides, they have high packaging capacity and low production cost. Niosomes are considered as a class of biodegradable cationic lipids which are made of the synthetic non-ionic surfactant, and they could be utilized for the delivery of high concentrations of therapeutic agents to tumor tissues (Hemati et al. 2019; Naderinezhad et al. 2017). Due to the cationic electrostatic charges found on the lipid bilayer, the loading efficiency of these carriers for nucleotides (possessing negative charges) would be acceptable, and the rate of cellular uptake of these molecules by the cells is notably high (Haghiralsadat et al. 2018a). In this study, a co-delivery system based on cationic PEGylated niosomes was developed to load miR-15a and miR-16–1 simultaneously on the surface of cationic PEGylated niosome against prostate cancer cell line (PC3).

Material and methods

Materials

Polysorbate 60 (Tween 60) and Sorbitan Monostearate 60(Span 60) were purchased from DaeJung Chemicals. 1,2-Distearoyl-phosphatidylethanolamine-methyl-polyethylene glycol-2000 (DSPE-mPEG 2000) was procured from Lipoid GmbH (Ludwigshafen, Germany). Cholesterol was obtained from Sigma-Aldrich Co (St. Louis, MO, USA) and N-[1-(2,3-Dioleoyloxy) propyl]-N,N,N-trimethyl ammonium methyl-sulfate (DOTAP) was purchased from Avanti Polar Lipids (Alabaster, AL). DAPI(4′,6-diamidino-2-phenylindole) and DIL Stain (1,1′-Dioctadecyl-3,3,3′,3′-Tetramethylindocarbocyanine Perchlorate) were purchased from Thermo Fisher (Waltham, Massachusetts, USA). Annexin V-FITC/PI apoptosis detection kit was supplied from Abcam (Abcam,Cambridge, UK). The mature sequences of miRNAs 15a/16–1 were obtained from the miR-Base database (http://mirbase.org). The sequences of hsa-miR15a were: sense 5′-UAGCAGCACAUAAUGGUUUGUG-3′, and hsa-miR16-1: sense 5′-CCAGUAUUAACUGUGCUGCUGA-3′. These oligonucleotides were synthesized via the fluorescent label CY-5 by Eurofins Genomics Company (Germany). Other Chemical and reagents were obtained from Sigma-Aldrich Chemical Co. (St. Louis, MO, USA).

Preparation of niosomal formulations

MicroRNAs loaded niosomes were synthesized and examined in terms of the particle size, polydispersity index (PDI), and zeta potential. For the optimization of niosomes, the following experiments were performed:

- The influence of surfactants with various hydrophobic tails and hydrophilic heads (tween 60 vs. span 60) on size and zeta potential of niosomes was evaluated.
- For increasing the lifetime of niosomes in the blood circulation and improving the drug bioavailability, 5% DSPE-PEG was added to the formulation of the prepared niosomes.
- After achieving the optimum conditions in terms of the particle size and zeta potential, 10%, 20%, and 25% DOTAP were added to PEGylated niosomes to facilitate the loading of oligonucleotides.

Different niosomal formulations were prepared by the thin-film hydration method. The percentage of surfactants in these formulations was 70%. As depicted in Table 1, various types of surfactants with different concentrations were dissolved in chloroform, as an organic phase, in the presence of 5% DSPE-mPEG and 30% cholesterol with or without phospholipids. The thin films were dried to remove chloroform by the rotary evaporator (Heidolph, Germany) at 45 °C. The dried lipid film was hydrated with PBS (phosphate-buffered saline) and rotated at 60 °C for 1 h. The niosomal dispersion was then sonicated for 20 min (10 s on and 10 s off, at an amplitude of 60 W) to minimize particle aggregation using ultrasonic homogenizer (model UP200St, Hielscher Ultrasonics GmbH, Germany). Finally, the dispersion was sterilized through 0.4 and 0.2 µm membrane filters. Non-modified niosomes were stored at 4 °C.

Preparation of cationic PEGylatedniosome (Nioplexes) containing miRNAs

In the post-coating stage (placing miRNAs on the surface of niosomes by the electrostatic interaction), miRNA/niosome complexes were prepared by the addition of miRNAs to the dispersion of PEGylated cationic niosomes at various weight ratios and then

Table 1 The effect of surfactant type and phospholipid on size, zeta potential and PDI

code	Tween60: Cholesterol	Span60: Cholesterol	DSPE-mPEG 2000 (%)	DOTAP	Size (nm)	Zeta potential (mV)	PDI (polydispersity index)
F1	–	70:30	5	–	134	− 45.46	0.28
F2	70:30	–	5	–	87	− 46.30	026
F3	70:30	–	5	10%	76	− 16.44	0.28
F4	70:30	–	5	20%	73	+ 5.31	0.33
F5	70:30	–	5	25%	69.7	+ 14.83	0.124

gently agitated by a vortex. Nioplexes, before using, were incubated at room temperature for 30 min to enhance the electrostatic interaction.

Determination of miRNA compilation with niosome and stability of Nioplexes

The loading efficiency of miRNA in cationic PEGylated niosomes was assessed using agarose gel retardation assay. In this assay, various ratios of niosome/oligonucleotide complexes were loaded on ethidium bromide-containing 1% agarose gel and then detected by electrophoresis at a voltage of 80 for 45 min. The images were obtained by UV exposure using a gel visualization system (Syngene GBOX, 680X), and they were analyzed in terms of the maximum loading efficiency for miRNA to be loaded on cationic PEGylate niosomes. For the determination of the stability, nioplexes suspensions were stored at 4 °C for four months and then the loading efficiency was evaluated.

Physical characterization of niosomal vesicles

Dynamic light scattering (DLS) was applied to determine the hydrodynamic size (diameter), polydispersity index (PDI), and size distribution of the designed nanocarriers. Zeta potential was also determined using Zeta Sizer Nano ZS apparatus (Malvern, Worcestershire, UK) to measure the surface charge of the synthesized nanocarriers. The structure and surface morphology of nanoniosomes were analyzed using scanning electron microscope (SEM) (model KYKY-EM3200-30 kV, KYKY Technology Development Ltd., Beijing, China) operated at accelerating voltage of 20 kV. For the preparation of samples used in the SEM analysis, a few drops of the niosome suspension were dispersed in water and placed on the mesh copper grid 400. Then, the grid was put in an evacuated desiccator to evaporate the solvent. Before being viewed under the microscope, the samples were sputter-coated with a thin layer of gold.

Cell lines and preparation of biological samples

Human adenocarcinoma prostate cell line (PC3) was procured from the Pasteur Institute, (Tehran, Iran), and immortalized human foreskin fibroblast cell line (HFF), as a normal cell line, was obtained from Stem Cell Biology Research Center (Yazd, Iran). All tissue culture media and supplies were obtained from Gibco (San Diego, California, US). PC3 and HFF cell lines were grown in the cell culture media of RPMI and DMEM, respectively. Both cell culture media were supplemented with 10% fetal bovine serum (FBS), and the cells were incubated at 37 °C in 5%CO_2 for 24 h.

Cytotoxicity assay

Cells were seeded in 96-well plates at a density of 5×10^3 cells per well and incubated for 24 h. Cells were then treated with free miR-15a (100, 200 nM), free miR-16–1 (100, 200 nM), miR-15a-loaded niosomes (100, 200 nM), miR-16–1-loaded niosomes (100, 200 nM),co-delivery of the free forms of miR-15a and miR-16–1, and co-delivery of miR-15a and miR-16–1 loaded on niosomes (nioplexe). HFF cells, which were applied as a normal cell line, were used to study the cytotoxicity of the unloaded niosomal formulations. After 48 h of incubation, the contents of wells were isolated and incubated with 20 µL MTT (5 mg/mL) for 4 h. Then, the medium was carefully aspirated and 150 µL DMSO (per well) was added to each well. The optical density of the samples was

measured at a wavelength of 570 nm for each well using the Synergy TMHT multi-mode microplate reader (Biotek Instruments Inc, USA).

Measurement of cellular uptake

PC3 cells were seeded in a 6-well plate at a density of 2×10^5 cells and then cultured at 37 °C until reached confluency 70%. Afterward, the cells were treated with unloaded niosomes, free miR-15a, free miR-16–1, miR-15a-loaded niosomes, miR-16–1-loaded niosomes, free complex of miR-15a/miR-16–1, and co-niosomal complex of miR-15a/miR-16–1(nioplexe). The designed complexes were prepared at a ratio of 1:10 and probed with Cy5/FAM-labeled miRNA and DIL/niosomes. The total concentration of miRNAs applied in each sample was kept constant at 100 nm. The treatment protocols were applied to cells and then incubated for 3 h. The cells were rinsed twice with PBS and fixed with 95% ethanol for 10 min. DAPI (0.125 μg/mL) was treated with the cells for 15 min to counterstain nuclei. The efficiency of cell transfection was investigated via the fluorescence intensity of CY-5/FAM and Dil. Images of the samples were observed by fluorescence microscopy (Olympus, Japan).

Real-time quantitative PCR (RT-PCR)

At first, 3×10^5 cells were seeded in 6-well plates, and then, the cells were transfected with unloaded niosome, free miR-15a (100 nM), free miR-16–1 (100 nM), miR-15a-loaded niosomes (100 nM), miR-16–1-loaded niosomes (100 nM), free complex of miR-15a / miR-16–1, and niosomal form of miR-15a/miR-16-(nioplexe)for 48 h. The total RNA was purified from PC3 cells by the means of the Trizol reagent (Invitrogen, Carlsbad, CA) according to the manufacturer commendations. The complementary DNA was produced by the High-Capacity cDNA Reverse Transcription Kit (Revert Aid First Strand cDNA Synthesis Kit, Thermo Scientific, USA). Real-time PCR amplification was performed using SYBR Premix Ex Taq II (Takara, Dalian) for 35 cycles based on the following protocol: 95 °C for5 min, 95 °C for 30 s, 60 °C for 30 s, 72 °C for 30 s, and 72°Cfor 5 min. The sequences of the primers were as follows: Bcl-2 sense: 5′-TGGGATGCCTTTGTGGAACTGTACG-3′; antisense 5′-GCCTGCAGCTTTGTTTCATGGTACA-3′; GAPDH sense 5′-TGCACCACCAACTGCTTAG C-3′; antisense5′-GGCATGGACTGTGGTCAT-GAG-3'.

Apoptosis assay

Cell apoptosis detection was carried out using Annexin V-FITC/PI staining. In brief, PC3 cells were seeded in a 48-well plate at a density of 2×10^4 cells and incubated until reached 80% confluency. Then, the cells were treated with free miRNAs, miRNA-loaded nanoniosomes, and the co-delivery of free miR-15a/miR-16–1 and co-delivery of miR-15a/miR-16–1 loaded niosome for 48 h. Afterward, the supernatant of the cell culture was discarded, and the cells were washed carefully with PBS buffer. Afterward, the cells were collected and resuspended in 100 μL binding buffer. Fluoresce isothiocyanate conjugated with Annexin V (2.5 μL) and propidium iodide (PI, 2.5 μL) were added to each sample, and the mixture was incubated in the dark at room temperature for 20 min. The cells were immediately counted by the flow cytometry analysis (Partech PASIII, Germany).

Statistical analysis

The statistical analysis was performed by one-way ANOVA, followed by Tukey's post hoc test for multiple comparisons. Student's t-test was used to compare two groups. The level of statistical significance was set at $p < 0.05$.

Results

The effect of surfactant on niosome formulations

For the determination of the optimal formulation to obtain the best small size (nanoscale), zeta potential, and PDI, various niosomal formulations were evaluated (Table1). As shown in Table1, the mean diameter of nanoniosomes containing tween 60 (F2) had a significantly lower smaller size as compared with nanoniosomes containing span 60 (F1). However, the zeta potential and PDI of these two formulations had no statistically significant difference. Notably, tween 60 has better stability in the hydration phase when incorporated into nanoniosome. Therefore, in this study, nanoniosome were made of tween 60.

The effect of phospholipids on niosomal formulations

In this study, cationic PEGylated nanoniosomes were developed that were capable of protecting miRNA against degradation, which is mediated by the nuclease accumulation in tumors. In this assay, to evaluate whether the molar ratio of DOTAP affects the particle size, PDI, and the surface charge of nanoniosome for miRNA adsorption, different amounts of DOTAP were added to produce cationic PEGylated nanoniosomal formulations. According to Table 1, the number of positive charge particles was increased upon the addition of DOTAP to F3-F5. Also, the vesicle size and PDI were declined linearly with the increase in the molar ratios of DOTAP. The obtained results showed that niosomal formulations containing Tween-60: cholesterol: DOTAP: DSPE-PEG2000 (F5) at molar ratios of 70:30:25:5 had the optimum characteristics in terms of the small diameter, zeta potential, and PDI (Table 1).

Characterization and determination of loading efficiency of nioplexes (miRNAs-loaded niosomes)

According to the results displayed in Table 2, the zeta-potential of the unloaded niosome is + 14.83 mV, while the incubation with miRNAs generally led to a decrease in zeta-potential and an increase in the size of vesicles. In all cases, PDI was less than 0.30, denoting the minimal aggregations. The loading of miRNAs on niosomes increased the diameter of both formulations, whereas it significantly reduced the zeta potential up to − 3.52 mV. The SEM analysis of nioplexes (Fig. 1) showed the spherical shapes with homogeneous size distribution. As expected, the mean diameter of nanoparticle was consistent with their size measured by the DLS method. In the assay performed on the interaction between miRNAs and noisome to assess the loading efficiency, the migration of miRNA-loaded niosomes on gel electrophoresis was much lower than free miRNAs (Fig. 2). The weight ratio of cationic PEGylated niosomes to miRNAs was calculated 10:1 to achieve the optimal condition.

Cytotoxicity assay

The MTT assay was performed to determine the cytotoxicity effects of different concentrations of unloaded niosome, free miR-15a,free miR-16–1, miR15a-loaded niosomes, miR16-1-loaded niosomes (100, 200 nM), the free complex of the two miRNAs, and niosomal forms of the two miRNAs on the growth of PC3 cells. A summary of experimental procedures for the measurement of cell death at 48 h is shown in Fig. 3 Nanoniosomes showed no significant cytotoxicity on the PC3 cell line up to a high concentration of 100 μg/mL. As shown in Fig. 3b, free forms of miRNAs had little cytotoxicity, while miRNAs loaded on niosomes had more toxicity than free miRNAs (p value < 0.05), indicating higher effectiveness of cationic niosomal formulations to deliver miRNA molecules. In this research, we indicated that co-delivery of miR-15a/miR-16–1 loaded on niosomes significantly reduced cell survival when compared with other formulations and demonstrated that the treatment with the free and the niosomal forms resulted in the growth inhibition of PC3 cells in a dose-dependent manner (p value < 0.05).

Cellular uptake assay

Figure 4 shows the cellular uptake of the free forms of miRNAs and miRNAs-loaded niosomes in PC3 cell lines after 3 h, monitored by fluorescence microscopy.

Table 2 Characterizations of the prepared niosomes

Optimal Formulation	Size (nm)	Zeta potential (mV)	PDI (polydispersity index)
Blank niosome	69.7	+ 14.83	0.124
miR15a-niosomal	99.5	+ 4.90	0.18
miR-16–1-niosomal	104	+ 3.36	0.15
CO-delivery miR-15a/miR16-1 niosomal	118.9	− 3.52	0.30

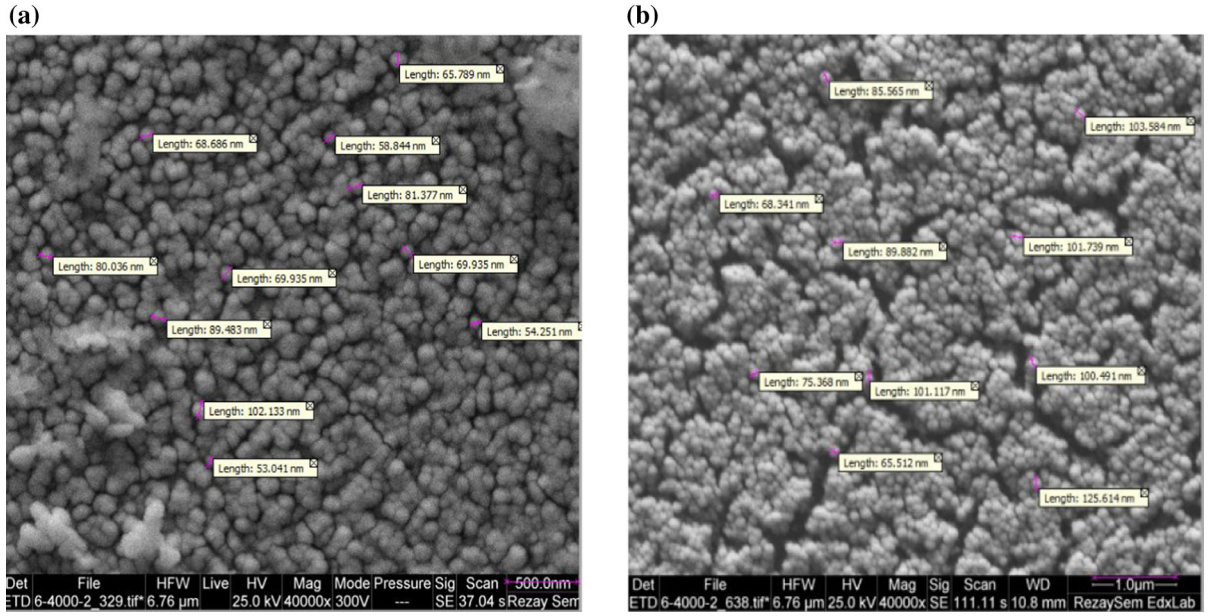

Fig. 1 Scanning electron microscopic (SEM) image of lipoplexes. **a** Blank niosome; **b** miR-15a/miR16-1 loaded niosome

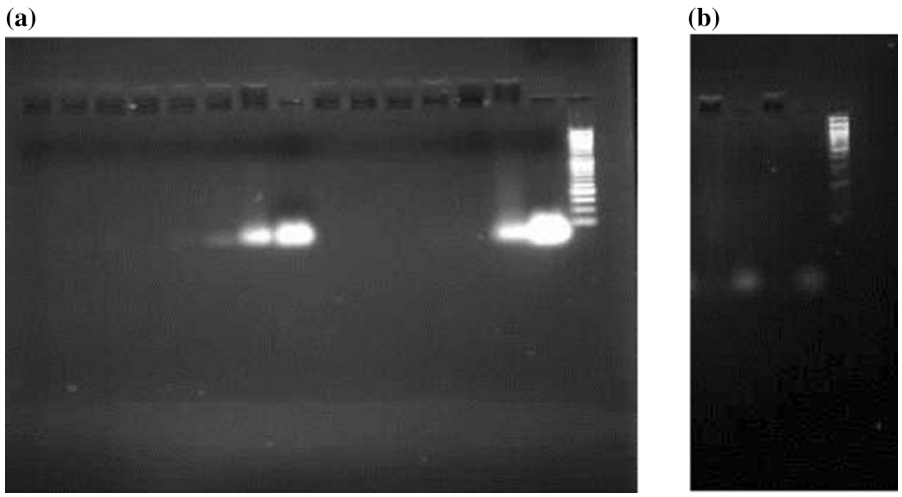

Fig. 2 **a** Agarose gel electrophoresis of free miRNA and miRNA loaded niosome vesicles to determine the most effective ratio of miRNA (µg): niosome (mg). Lane 1 = DNA ladder; lane 2 and 9 = free miRNA 15-a and free miRNA 16–1 (0.5 µL), respectively; lane 3 and 10 = lipoplex (1.5 µL niosome, 0.5 µL miRNA); lane 4 and 11 = lipoplex (5 µL niosome, 0.5 µL miRNA); lane 5 and 12 = lipoplex (10 µL niosome, 0.5 µL miRNA); lane 6 and 13 = lipoplex (12.5 µL niosome, 0.5 µL miRNA); lane 7 and 14 blank niosome (5 µL). **b** Monitoring of miRNA loading stability after four months storage at 4 °C, Lane 1 = DNA ladder; lane 2 and 4 = free miRNA 15-a and free miRNA 16–1, respectively (0.5 µl); lane 3 and 5 = lipoplex (5 µL niosome, 0.5 µL miRNA 15-a and miRNA 16–1, respectively)

Figure 4 depicts the successful delivery of DIL-labeled niosomes to cancer cells. These results suggest that niosomes substantially improve cellular uptake with the minimum cytotoxicity. Free miRNAs showed lower cellular uptake efficiency, as the total intensity of fluorescent labels was noticeably diminished. The results indicated that miRNAs loaded niosomes had a higher rate of cellular uptake and showed greater purple and turquoise blue color intensity compared with cells treated with free forms of miRNAs. The

combination of miR15a-/miR16-1 loaded niosomes showed the highest percentage of cellular uptake and the mean fluorescence intensity when compared with other formulations. The positive charge of the niosome surface exhibited a marginal increase in the efficiency of cellular uptake in PC3 cells.

Fig. 4 Fluorescent microscopic analysis of uptake of free miRNAs, Blank niosome, and lipoplexes 3 h after transfection. Cell nuclei were stained with DAPI (blue), and transfected cells were fixed with 4% paraformaldehyde (×60 magnification). **b** Fluorescence intensities were calculated by ImageJ and plotted as mean fluorescence intensity. *p < 0.05

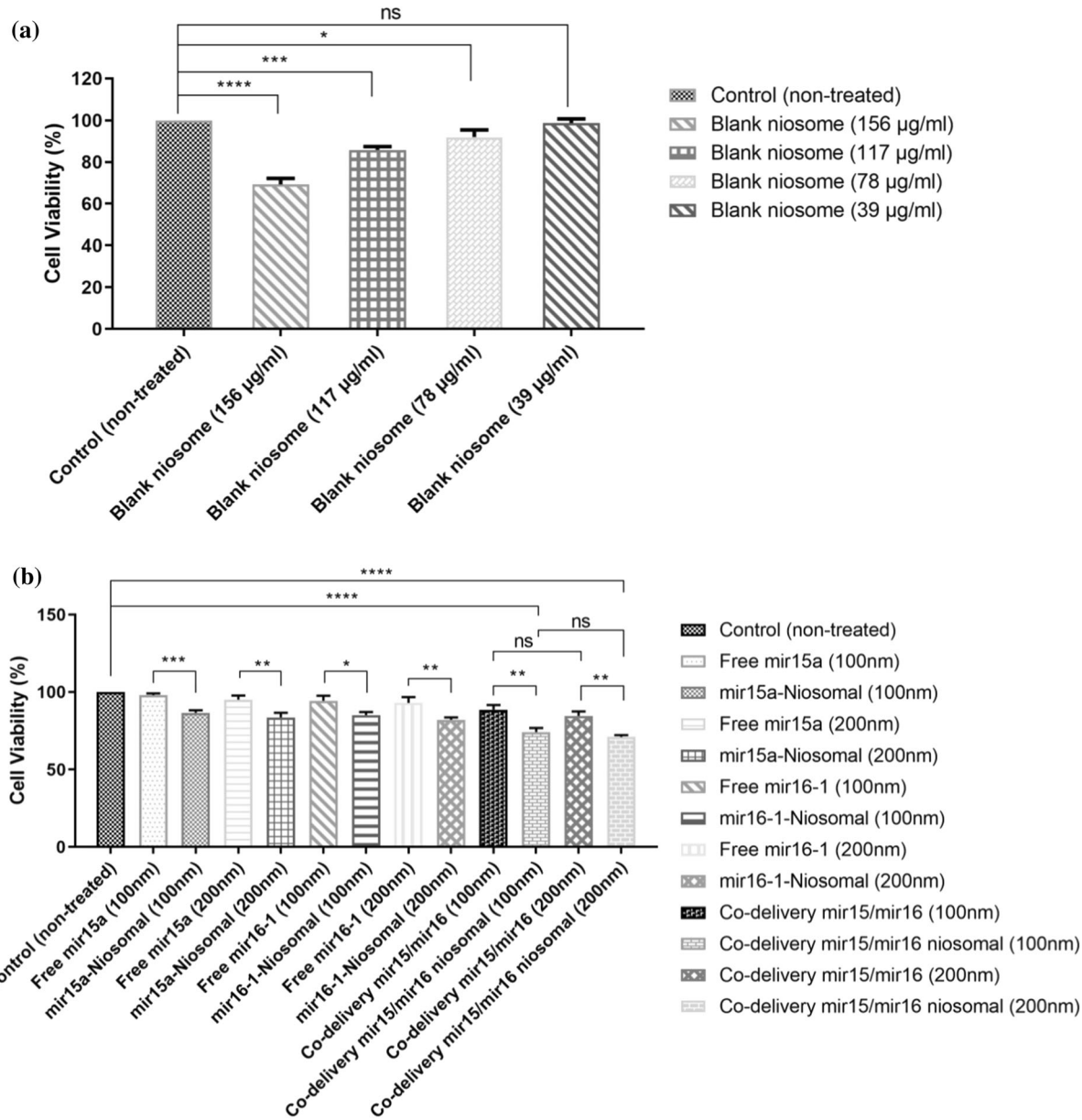

Fig. 3 Evaluation of cell viability percentage **a** blank niosome; **b** free miRNAs and lipoplexes. The values were expressed as mean ± SD from three independent experiments. *p < 0.05, **p < 0.01, ***p < 0.001, ****p < 0.0001, ns (non-significant)

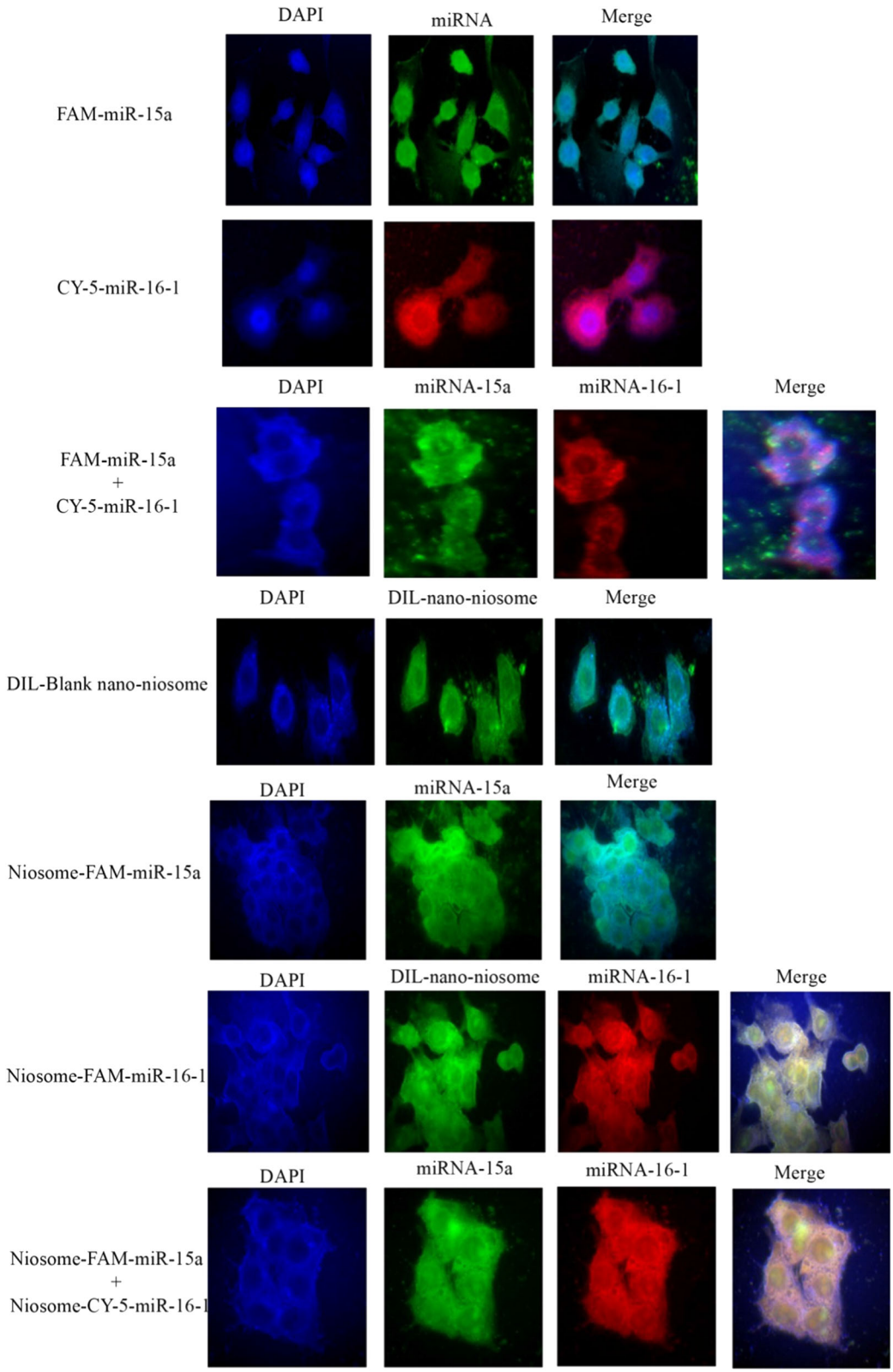
DAPI
miRNA
Merge
FAM-miR-15a
CY-5-miR-16-1
DAPI
miRNA-15a
miRNA-16-1
Merge
FAM-miR-15a
+
CY-5-miR-16-1
DAPI
DIL-nano-niosome
Merge
DIL-Blank nano-niosome
DAPI
miRNA-15a
Merge
Niosome-FAM-miR-15a
DAPI
DIL-nano-niosome
miRNA-16-1
Merge
Niosome-FAM-miR-16-1
DAPI
miRNA-15a
miRNA-16-1
Merge
Niosome-FAM-miR-15a
+
Niosome-CY-5-miR-16-1

Decreased expression of Bcl-2 in therapeutic protocols

The transfection efficiency of the combinatory use of miR15a/miR16-1 loaded niosomes, the expression of the Bcl-2 gene was assayed in prostate cancer cell line 48 h after the transfection (Fig. 5). According to Fig. 5, it was found that 100 nM miRNAs remarkably reduced the expression of Bcl-2 at the transcription level after 48 h when compared with the cells treated with unloaded niosomes. Furthermore, miRNA loaded niosome markedly decreased the expression of Bcl-2 significantly at the transcription level as compared to the free forms. Moreover, cells transfected with the combination of the niosomal form of miR15a-/miR16-1 complex showed a significant reduction in Bcl-2 expression compared with cells transfected with miR15a- and miR16-1-loaded niosomes alone. All in all, these results indicate that the synthesized niosomal complexes have great potential to inhibit the expression of the Bcl-2 gene, thereby inhibiting the cell proliferation of prostate cancer cells.

Apoptosis analysis

The apoptosis rate was 4.38% and 4.14% in cells treated with the free forms of miR15a and miR16-1, respectively. However, the rate of apoptosis was increased to 11.1% and 8.98% when the cells treated with miR15a- and miR16-1-loadedniosomes, respectively. Furthermore, there was a significant increase in the rate of cell death (34.4%) when the cells were simultaneously treated withmiR15a-/miR16-1-loaded niosomes. The combinatory usage of the two miRNAs in the form of niosomes had a synergistic effect on the induction of apoptosis in comparison with the application of free forms of miR15a and miR16-1. These results are consistent with the cytotoxicity assay (Fig. 6).

Discussion

The use of therapeutic miRNAs to quench genes responsible for the development of drug resistance has been broadly employed as a promising strategy to oppress the expression of oncogenes, which blame for the abnormal proliferation of cancer cells (Zhou et al. 2017).Given the benefits of miRNAs, such as high efficiency, specificity, and low toxicity, the application of these molecules is widely utilized in gene therapy (Bai et al. 2019). In addition to the regulatory roles of miRNA in cellular processes, they are useful for diagnostic and therapeutic purposes (Huang 2017).

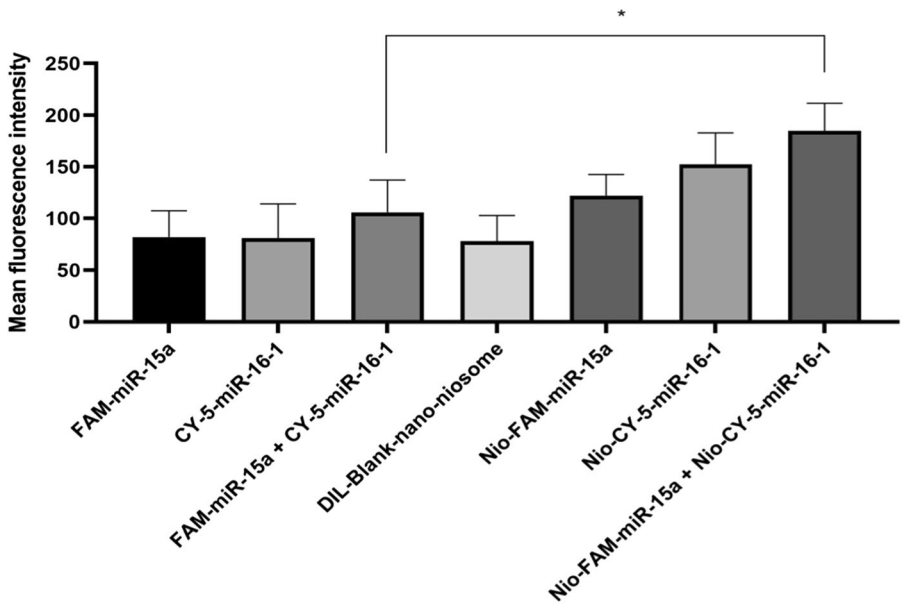

Fig. 5 Real-time PCR analysis of Bcl2 mRNA level in PC3 cells transfected by different niosomes. The values were expressed as mean ± SD from three independent experiments. *$p < 0.05$, ****$p < 0.0001$

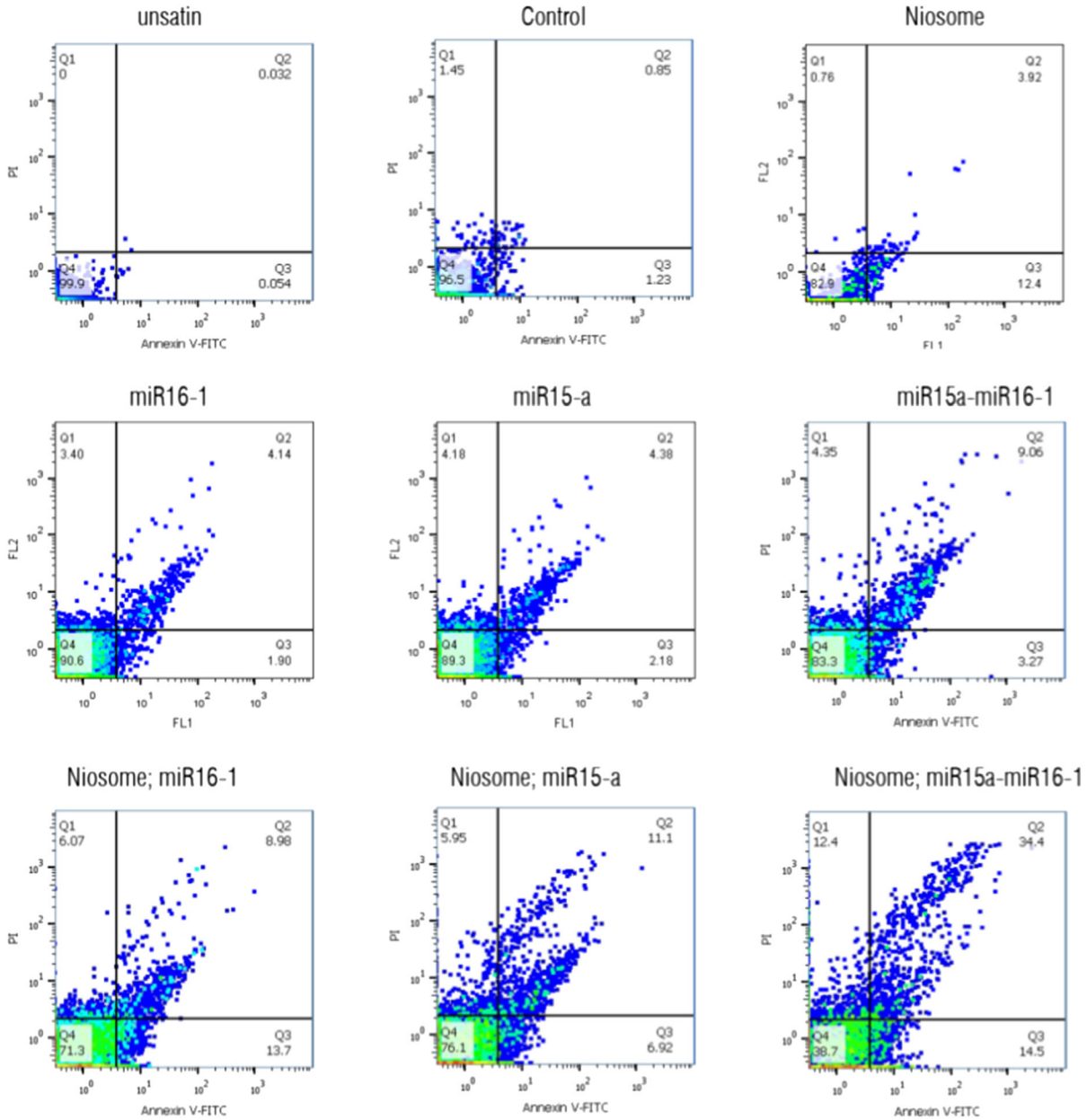

Fig. 6 Cell apoptosis analyzed with Annexin V-FITC kit following the treatment of cells for 48 h

MiR15a and miR16-1 have been shown to be frequently deleted or downregulated in B-CLL and prostate cancer (Bonci et al. 2008; Chen et al. 2006). These miRNAs modulate the expression of some oncogenes, such as BCL-2 and MCL1. A recent study reported that the overexpression of miR-15a and miR-16–1 inhibits the growth of prostate cancer cells by targeting the anti-apoptotic Bcl-2 gene (Bonci et al. 2008). The therapeutic index of miR-15a and miR-16–1 in cancer therapy is considered as a challenge. Due to the instability of miRNAs and their negative charge, they would be rapidly degraded in the systemic circulation and therefore have low cellular uptake by cancer cells. Thus, an unique approach is highly required to protect miRNAs against degradation and facilitates the delivery of them to tumor cells

with high loading efficiency. Several strategies have been applied to deliver miRNAs into tumor cells. In previous reports, miRNAs were primarily delivered by viral and non-viral vectors for the transfection process (Yang 2015). Lipid-based vectors are also widely employed as non-viral carriers. In the present study, a niosomal formulation was designed by the addition of the following components: (i) Tween 60, a non-ionic surfactant (ii) DOTAP, a cationic lipid (iii) Cholesterol, a helper lipid (iv) DSPE-PEG, a surface coating lipid. The formulation presented in this study is a novel approach for the treatment of prostate adenocarcinoma and other cancers based on the evaluation of toxicity and selectivity. Cationic PEGylated niosomes showed the average size less than 100 nm and they had high cellular uptake, stable structure, and no toxicity. The combination of miRNAs (e.g., miR-15a and miR-16–1) to target a particular cancer-related pathway could have potent effects on the indication of programmed cell death than the use of miRNAs alone. In this study, we established a novel and optimized delivery system made of PEGylated cationic niosomes to be able to simultaneously delivery two tumor suppressor miRNAs (miR15a and miR16-1) to prostate cancer cells. The results of the MTT assay indicated that the survival of PC3 cells was significantly reduced when treated with niosomal miR-15a/miR-16–1 in comparison with other treatments, suggesting the inhibitory role of these two miRNAs in the proliferation of prostate cancer cells. This event confirms that the exogenous application of miR-15a and miR-16–1 can markedly impede the cell proliferation of PC3 cell line which is consistent with similar studies showing the inhibitory roles of these two miRNAs in the hindrance of cancer cells in various malignancies. Sambri et al. demonstrated that the transfection of hepatocellular carcinoma cells (HepG2) with miR-15a and miR-16–1 could prevent the cell growth of this type of cancer cells. They used precursor molecules mimicking microRNA 15a (pre-miR-15a), microRNA 16–1 (pre-miR-16–1) to transfect HepG2 cells with TRANSIT-TKO Transfection Reagent. They also found that the cells transfected with RNAi mimicking molecules have significantly decreased the tumor growth of HepG2 cells (Sambri et al. 2011). Bcl-2, as an anti-apoptotic protein, plays an essential role in the process of apoptosis. The regulation of this protein is disrupted in various types of cancers, and its functions in the development and etiology of cancer remain controversial (Campbell and Tait 2018). Bcl-2 has also shown oncogenic function and increases tumorigenesis in different animal models used for the study of cancer (Albamonte et al. 2008). In this study, the qRT-PCR technique was utilized to evaluate the expression level of Bcl-2 after the transfection of PC3 cells with miR-15a and miR-16–1, which were loaded in cationic niosomes. The results of the assay showed that the expression of Bcl-2 at the mRNA level was diminished after the transfection of PC3 cells with miR-15a and miR-16–1 and these Exogenous miRNAs appear to be able to decrease Bcl-2 expression. Co-transfection of niosomal forms of miR-15a/miR16-1 was more effective in reducing Bcl-2 gene expression in PC3 cells. Also, the inhibition of cell growth with combined therapy was more pronounced than using the free forms of miR-15a and miR16-1, or even the single usage of each miR-15a-and miR-16–1-loaded nanoniosomes. Also, increased expression of miRNA-15a and miR-16–1 decreased the level of Bcl-2 and increased the rate of cell death. These findings were consistent with the results of Bonic et al., who studied the expression of Bcl-2 in prostate cancer cells. They reported that the suppression of the expression of Bcl-2 by the overexpression of miR-15a and miR-16–1 in prostate cancer cells led to a decrease in cell proliferation, invasion of cancer cells to surrounding tissues, and metastasis of prostate tumor xenografts. Their results proposed that miR-15a and miR-16 act as tumor suppressor genes in prostate cancer through the control of cell survival, proliferation, and invasion (Bonci et al. 2008). In 2013, Li and colleagues used a combination of Bcl-2 small interfering RNA (siRNA) with miR-15a oligonucleotides against the Bcl-2 protein that led to the induction of cell apoptosis in Raji cells and therapy of B-Cell lymphoma. Their results showed a significant change in the gene expression of Bcl-2, cell viability, and apoptosis when compared with the control treatment (Ding et al. 2013). In the present study, the anti-cancer properties of miR-15a and miR-16–1 were confirmed in PC3 cells. Cimmino et al. demonstrated that the expression levels of miR-15a and miR-16–1 are conversely associated with Bcl2 expression in CLL and they negatively regulate Bcl-2 at a posttranscriptional level. They are natural antisense Bcl-2 molecules that are employed for the elimination of Bcl-2-overexpressing tumors (Cimmino et al. 2005). Xia et al.

indicated that the downregulation of miR-15b and miR-16 in gastric cancer cells concurrently occurs with the upregulation of Bcl-2 protein. The overexpressed miR-15b or miR-16 can diminish the protein level of Bcl-2 and play a role in the treatment of gastric cancer (Xia et al. 2008). Their results were consistent with this study findings. Several studies have shown that the anti-apoptotic protein MCL-1 belonging to the Bcl-2 family is another target of miR-15a and miR-16–1 (Liu et al. 2014). Other studies have demonstrated that miR-15a and miR-16–1 can inhibit the cell cycle and inhibit proliferation in osteosarcoma cells (Cai et al. 2012). In another study, the inhibitory role of miR-15a and miR-16–1 in the process of angiogenesis in multiple myeloma was studied in which the two miRNAs mentioned earlier can target the VEGF protein (Sun et al. 2013). It has been reported that the anti-apoptotic proteins MCL-1 and CCND1 are direct targets of both miR-15a and miR-16–1. Targeting these miRNAs enhances the expression of the pro-apoptotic Bim protein, which ultimately induces apoptosis. Therefore, according to previous studies, the presence of exogenous miR-15a and miR-16–1 regulates the mediators of the mitochondrial apoptosis pathway in PC3 cells through a decrease in the expression of Bcl-2, eventually leading to the prevention of the cell proliferation and induction of cell death.

Conclusions

Our results revealed that the co-delivery of miR-15a and miR-16–1 loaded niosomes exerts synergistic anti-cancer potentials when utilized in-vitro. The particle size and zeta potentials of the designed co-delivery system were suitable to be used as they had high cellular uptake due to the electrostatic interactions with the cell membrane. The combination of miR-15a and miR-16–1 provides a new platform for combination therapy to induce apoptosis and decrease the expression of the Bcl-2 protein. Therefore, this co-delivery system can open up a new horizon for the treatment of prostate cancer.

Compliance with ethical standards

Conflict of interest No potential conflict of interest was reported by the authors.

References

Acunzo M, Croce CM (2016) Downregulation of miR-15a and miR-16–1 at 13q14 in chronic lymphocytic leukemia. Clin Chem 62:655–656. https://doi.org/10.1373/clinchem.2015.240036

Albamonte MS, Willis MA, Albamonte MI, Jensen F, Espinosa MB, Vitullo AD (2008) The developing human ovary: immunohistochemical analysis of germ-cell-specific VASA protein, BCL-2/BAX expression balance and apoptosis. Human Reprod 23:1895–1901

Aqeilan R, Calin G, Croce C (2009) Aqeilan RI, Calin GA, Croce CM. miR-15a and miR-16–1 in cancer: discovery, function and future perspectives. Cell Death Differ 17:215–220. https://doi.org/10.1038/cdd.2009.69

Aqeilan RI, Calin GA, Croce CM (2010) miR-15a and miR-16–1 in cancer: discovery, function and future perspectives. Cell Death Differ 17:215–220. https://doi.org/10.1038/cdd.2009.69

Bai Z et al (2019) Non-viral nanocarriers for intracellular delivery of microRNA therapeutics. J Mater Chem B 7:1209–1225. https://doi.org/10.1039/C8TB02946F

Bandi N et al (2009) miR-15a and miR-16 are implicated in cell cycle regulation in a Rb-dependent manner and are frequently deleted or down-regulated in non–small cell lung cancer. Cancer Res 69:5553–5559

Baraban JM, Shah A, Fu X (2018) Chapter one - multiple pathways mediate microRNA degradation: focus on the translin/trax RNase complex. In: Pasternak GW, Coyle JT (eds) Advances in pharmacology, vol 82. Academic Press, New York, pp 1–20

Bonci D et al (2008) The miR-15a–miR-16–1 cluster controls prostate cancer by targeting multiple oncogenic activities. Nat Med 14:1271. https://doi.org/10.1038/nm.1880

Cai CK et al (2012) miR-15a and miR-16–1 downregulate CCND1 and induce apoptosis and cell cycle arrest in osteosarcoma. Oncol Rep 28:1764–1770. https://doi.org/10.3892/or.2012.1995

Campbell KJ, Tait SWG (2018) Targeting BCL-2 regulated apoptosis in cancer. Open Biol 8:180002. https://doi.org/10.1098/rsob.180002

Chen L, Tang L, Calin G, Croce CM, Kipps TJ (2006) Expression of microRNA (miR) miR-15a/miR-16–1 downregulates expression of BCL-2 protein in chronic lymphocytic leukemia. Blood 108:2796–2796. https://doi.org/10.1182/blood.V108.11.2796.2796

Cimmino A et al (2005) miR-15 and miR-16 induce apoptosis by targeting BCL2. Proc Natl Acad Sci U S A 102:13944–13949. https://doi.org/10.1073/pnas.0506654102

Ding L, Hu X-M, Wu H, Liu G-X, Gao Y-J, He D-M, Zhang Y (2013) Combined transfection of Bcl-2 siRNA and miR-15a oligonucleotides enhanced methotrexate-induced apoptosis in Raji cells. Cancer Biol Med 10:16

Guo WT, Wang Y (2019) Dgcr8 knockout approaches to understand microRNA functions in vitro and in vivo. Cell Mol Life Sci 76:1697–1711. https://doi.org/10.1007/s00018-019-03020-9

Haghiralsadat F, Amoabediny G, Helder MN, Naderinezhad S, Sheikhha MH, Forouzanfar T, Zandieh-Doulabi B (2018a)

A comprehensive mathematical model of drug release kinetics from nano-liposomes, derived from optimization studies of cationic PEGylated liposomal doxorubicin formulations for drug-gene delivery. Artif Cells Nanomed Biotechnol 46:169–177. https://doi.org/10.1080/21691401.2017.1304403

Haghiralsadat F, Amoabediny G, Naderinezhad S, Forouzanfar T, Helder MN, Zandieh-Doulabi B (2018b) Preparation of PEGylated cationic nanoliposome-siRNA complexes for cancer therapy. Artif Cells Nanomed Biotechnol 46:684–692. https://doi.org/10.1080/21691401.2018.1434533

Haghiralsadat F, Amoabediny G, Naderinezhad S, Zandieh-Doulabi B, Forouzanfar T, Helder MN (2018c) Codelivery of doxorubicin and JIP1 siRNA with novel EphA2-targeted PEGylated cationic nanoliposomes to overcome osteosarcoma multidrug resistance. Int J Nanomed 13:3853–3866. https://doi.org/10.2147/ijn.S150017

Hemati M, Haghiralsadat F, Jafary F, Moosavizadeh S, Moradi A (2019) Targeting cell cycle protein in gastric cancer with CDC20siRNA and anticancer drugs (doxorubicin and quercetin) co-loaded cationic PEGylated nanoniosomes. Int J Nanomed 14:6575–6585

Hsu S-h et al (2013) Cationic lipid nanoparticles for therapeutic delivery of siRNA and miRNA to murine liver tumor. Nanomed Nanotechnol Biol Med 9:1169–1180

Huang W (2017) MicroRNAs: biomarkers, diagnostics, and therapeutics. Methods Mol Biol (Clifton, NJ) 1617:57–67. https://doi.org/10.1007/978-1-4939-7046-9_4

Kang W et al (2015) Targeting of YAP1 by microRNA-15a and microRNA-16–1 exerts tumor suppressor function in gastric adenocarcinoma. Mol Cancer 14:52

Kopper L, Tímár J (2005) Genomics of prostate cancer: Is there anything to „translate"? Pathol Oncol Res 11:197–203. https://doi.org/10.1007/BF02893851

Liu J et al (2014) Loss of p53 and altered miR15-a/16–1 MCL-1 pathway in CLL: insights from TCL1-Tg: $p53^{-/-}$ mouse model and primary human leukemia cells. Leukemia 28:118

Naderinezhad S, Amoabediny G, Haghiralsadat F (2017) Co-delivery of hydrophilic and hydrophobic anticancer drugs using biocompatible pH-sensitive lipid-based nano-carriers for multidrug-resistant cancers RSC. Advances 7:30008–30019. https://doi.org/10.1039/C7RA01736G

Palanichamy JK, Rao DS (2014) miRNA dysregulation in cancer: towards a mechanistic understanding. Front Genet 5:54–54. https://doi.org/10.3389/fgene.2014.00054

Patel N, Garikapati KR, Ramaiah MJ, Polavarapu KK, Bhadra U, Bhadra MP (2016) miR-15a/miR-16 induces mitochondrial dependent apoptosis in breast cancer cells by suppressing oncogene BMI1. Life Sci 164:60–70. https://doi.org/10.1016/j.lfs.2016.08.028

Pejin B, Jovanovic KK, Mojovic M, Savic AG (2013) New and highly potent antitumor natural products from marine-derived fungi: Covering the period from 2003 to 2012. Curr Top Med Chem 13:2745–2766

Pejin B, Jovanovic KK, Savic AG (2015) New antitumour natural products from marine red algae: covering the period from 2003 to 2012. Mini Rev Med Chem 15:720–730

Porkka KP et al (2011) The miR-15a-miR-16-1 locus is homozygously deleted in a subset of prostate cancers. Genes Chromos Cancer 50:499–509

Qian H, Tay CY, Setyawati MI, Chia SL, Lee DS, Leong DT (2017) Protecting microRNAs from RNase degradation with steric DNA nanostructures. Chem Sci 8:1062–1067. https://doi.org/10.1039/c6sc01829g

Sambri I, Capasso R, Pucci P, Perna AF, Ingrosso D (2011) The microRNA 15a/16–1 cluster down-regulates protein repair isoaspartyl methyltransferase in hepatoma cells: implications for apoptosis regulation. J Biol Chem 286:43690–43700. https://doi.org/10.1074/jbc.M111.290437

Sun CY et al (2013) miR-15a and miR-16 affect the angiogenesis of multiple myeloma by targeting VEGF. Carcinogenesis 34:426–435. https://doi.org/10.1093/carcin/bgs333

Xia L et al (2008) miR-15b and miR-16 modulate multidrug resistance by targeting BCL2 in human gastric cancer cells. Int J Cancer 123:372–379. https://doi.org/10.1002/ijc.23501

Yang N (2015) An overview of viral and nonviral delivery systems for microRNA. Int J Pharm Investig 5:179–181. https://doi.org/10.4103/2230-973X.167646

Zhang XJ, Ye H, Zeng CW, He B, Zhang H, Chen YQ (2010) Dysregulation of miR-15a and miR-214 in human pancreatic cancer. J Hematol Oncol 3:46

Zhou K, Liu M, Cao Y (2017) New insight into microRNA functions in cancer: oncogene-microRNA-tumor suppressor gene network. Front Mol Biosci 4:46–46. https://doi.org/10.3389/fmolb.2017.00046

Zhu C-S, Zhu L, Tan D-A, Qiu X-Y, Liu C-Y, Xie S-S, Zhu L-Y (2019) Avenues toward microRNA detection in vitro: a review of technical advances and challenges. Comput Struct Biotechnol J 17:904–916. https://doi.org/10.1016/j.csbj.2019.06.018